The Influence of WSR-88D Intra-Volume Scanning Strategies on Thunderstorm Observations and Warnings in the Dual-Polarization Radar Era: 2011–20

DARREL M. KINGFIELD[a,b] AND MICHAEL M. FRENCH[c]

[a] *Cooperative Institute for Research in Environmental Sciences, University of Colorado Boulder, Boulder, Colorado*
[b] *NOAA/Global Systems Laboratory, Boulder, Colorado*
[c] *School of Marine and Atmospheric Sciences, Stony Brook University, State University of New York, Stony Brook, New York*

(Manuscript received 30 July 2021, in final form 12 October 2021)

ABSTRACT: The Weather Surveillance Radar-1988 Doppler (WSR-88D) network has undergone several improvements in the last decade with the upgrade to dual-polarization capabilities and the ability for forecasters to rescan the lowest levels of the atmosphere more frequently through the use of Supplemental Adaptive Intra-volume Scanning (SAILS). SAILS reduces the revisit period for scanning the lowest 1 km of the atmosphere but comes at the cost of a longer delay between scans at higher altitudes. This study quantifies how often radar volume coverage patterns (VCPs) and all available SAILS options are used during the issuance of 148 882 severe thunderstorm and 18 263 tornado warnings, and near 10 474 tornado, 58 934 hail, and 127 575 wind reports in the dual-polarization radar era. A large majority of warnings and storm reports were measured with a VCP providing denser low-level sampling coverage. More frequent low-level updates were employed near tornado warnings and reports compared to severe thunderstorm warnings and hail or wind hazards. Warnings issued near a radar providing three extra low-level scans (SAILSx3) were more likely to be verified by a hazard with a positive lead time than warnings with fewer low-level scans. However, extra low-level scans were more frequently used in environments supporting organized convection as shown using watches issued by the Storm Prediction Center. In recent years, the number of midlevel radar elevation scans is declining per hour, which can adversely affect the tracking of convective polarimetric signatures, like Z_{DR} columns, which were found above the lowest elevation angle in over 99% of cases examined.

KEYWORDS: Severe storms; Radars/Radar observations; Forecasting techniques

1. Introduction

For over two decades, the Next Generation Weather Radar (NEXRAD) program's Weather Surveillance Radar-1988 Doppler (WSR-88D) network has collected data on atmospheric phenomena across the United States and selected sites abroad (Crum et al. 1998). Its installation and associated forecaster training program revolutionized the detection of hazardous weather and led directly to significant improvements in severe weather warning performance when compared to the pre-NEXRAD era (Polger et al. 1994; Bieringer and Ray 1996). Its benefits were emphasized in a National Academy of Sciences (2002) report where it was concluded that "weather radar has become the primary means of detecting, describing, tracking, and nowcasting or forecasting precipitation-laden and, to a more limited extent, clear air weather over the contiguous United States."

To collect measurements of the atmosphere, the WSR-88D uses volume coverage patterns (VCPs), which control the antenna rotation rate, scanning elevation angles (i.e., the angle relative to the radar horizon), and pulse repetition frequency (Crum et al. 1993). Initially, the WSR-88D came with four VCPs, two for sampling precipitating systems and two for clear air surveillance, which scan each elevation angle 360° in contiguous order away from the ground to create a "volume" of data. Each VCP has its own strengths and limitations; Maddox et al. (1999) noted that the two initial precipitation VCPs have coverage gaps between elevation angles starting at 25 km away from the radar, resulting in degraded vertical sampling of the atmosphere beyond this range. To continuously evolve the science and technology of the WSR-88D, the NEXRAD Product Improvement Program was established to coordinate and oversee hardware and software enhancements for the network (Crum et al. 1998; Saffle et al. 2002). This program has led to many notable improvements including new radar data sources and access to additional precipitation VCPs (e.g., Brown et al. 2005; Zittel and Wiegman 2005; Istok et al. 2009), signal processing and data quality improvements (e.g., Torres and Curtis 2007; Hubbert et al. 2009; Ice et al. 2013), and new algorithms (Smalley et al. 2005; Ryzhkov et al. 2013; Snyder and Ryzhkov 2015; Krause 2016; Richardson et al. 2017).

Natural disasters can also drive radar improvements, the NOAA (2011) Service Assessment for the 22 May 2011 Joplin, Missouri, EF5 tornado recommended the National Weather Service (NWS) "develop and implement additional hybrid WSR-88D VCP strategies that allow for more continuous sampling near the surface (e.g., 1-minute lowest elevation sampling)." Before this service assessment, work was already ongoing to provide faster volumes of radar data. In the fall of 2011, the Automated Volume Scan Evaluation and Termination (AVSET; Chrisman 2009) software update was activated at all sites. AVSET works by terminating a volume scan early if there are no significant radar returns (i.e., the beam overshoots the anvil of a storm far away from the radar) and drops

Corresponding author: Darrel M. Kingfield, darrel.kingfield@noaa.gov

DOI: 10.1175/WAF-D-21-0127.1

down to the lowest elevation angle sooner. While beneficial for distant and/or shallow convection, the coverage and depth of thunderstorms during outbreak events may not allow for AVSET to be triggered.

To inject more low-level scans into a volume, three other optional strategies attached to a VCP were implemented: Supplemental Adaptive Intra-volume Low-Level Scanning (SAILS), Multiple Elevation Scan Option SAILS (MESO-SAILS), and Mid-Volume Rescan of Low-Level Elevations (MRLE). SAILS revisits the lowest elevation angle, usually 0.5° above the radar horizon for most sites, once in the middle of the volume scan, resulting in at least 71% more low-level scans per hour (Chrisman 2013). MESO-SAILS allows for the 0.5° elevation angle to be revisited up to three additional times per volume, lowering the average revisit time for 0.5° scans from 256 to 89 s (Daniel et al. 2014; Istok et al. 2017). MRLE allows for the revisit of 2–4 low-level scan angles (0.5°, 0.9°, 1.3°, and 1.8°) (Chrisman 2016). All three strategies can greatly improve the interrogation of rapidly evolving low-level signatures like those seen in severe convection; however, it comes with the caveat of slower revisit intervals at higher elevation angles. For example, at 19.5°, the highest elevation angle of a WSR-88D, the revisit time is delayed from 243 to 336 s when MESO-SAILS with four total 0.5° elevation angles are added (Chrisman 2014).

While low-level scanning coverage and frequency is beneficial for diagnosing low-level hazards (e.g., tornadoes), an examination of thunderstorm characteristics aloft using traditional radar moment data can show precursor signatures for other threats that can cause widespread damage and impact aviation operations. Eilts et al. (1996) examined 85 storms and identified deep convergence at midlevels and descending reflectivity cores as common observations prior to downburst events. Witt et al. (1998a) emphasized heights above the −20°C isothermal level as the optimal hail growth region when developing the WSR-88D hail detection algorithm. Deierling and Petersen (2008) found that updraft volume, particularly above the −5°C isothermal level, correlated the best with total lightning activity.

The upgrade of the nationwide WSR-88D network to dual-polarization capabilities from 2011 to 2013 offered forecasters and researchers new tools to scrutinize convective storms. Repeatable, even ubiquitous, polarimetric signatures in convective storms are known to indicate ongoing dynamic, thermodynamic, and/or microphysical processes. The presence of these signatures and/or their physical characteristics or magnitudes may be used as proxies for storm features and allow forecasters to infer important storm processes that may improve convective nowcasting skill. Some of these polarimetric signatures occur at storm mid- to upper levels, most notably the differential reflectivity (Z_{DR}) and specific differential phase (K_{DP}) columns consisting of elevated values of each field owing to lofting of raindrops above the freezing level (e.g., Illingworth et al. 1987; Hubbert et al. 1998; Kumjian and Ryzhkov 2008; Kumjian et al. 2014; van Lier-Walqui et al. 2016); these features can therefore serve as markers for storm updrafts. In turn, it has been demonstrated that Z_{DR} columns may be used to nowcast hail (Picca et al. 2010), improve severe storm identification (Kuster et al. 2019), and even predict peak tornado intensity (French and Kingfield 2021). The identification of K_{DP} cores may be used in convective nowcasting, particularly for downburst prediction (Kuster et al. 2021). Also, near-zero Z_{DR} and widespread low values of ρ_{HV} aloft coincident with or downwind of a tornado indicate debris or debris fallout (e.g., Ryzhkov et al. 2005; Houser et al. 2015; Kurdzo et al. 2015). The height of the debris signature may even be used in near–real time to estimate tornado intensity (e.g., Gibbs 2016; Emmerson et al. 2019). The identification and monitoring of trends in thunderstorm signatures at both mid and low-levels on radar can provide a forecaster with confidence in issuing a warning and conveying the appropriate threat in the message to the public (Bowden et al. 2015; Bowden and Heinselman 2016).

NWS offices have been able to activate SAILS since 2014, MESO-SAILS since 2015, and MRLE since 2018. Some WSR-88D sites gained dual-polarization capabilities in 2011, but most sites started using intra-volume scanning strategies 12–18 months after this upgrade. Therefore, most polarimetric radar observations are subject to a longer delay between scans at mid- to upper levels. A time delay could be particularly troublesome for algorithms designed to ingest and blend data from multiple radars and create decision-assistance products, such as the Multi-Radar Multi-Sensor (MRMS) system that supports NWS operations (Zhang et al. 2016; Smith et al. 2016). As a result, it is important to determine if the trade-off of additional low-level scans for fewer scans aloft are beneficial in the warning process. In addition, as already summarized, there are an increasing number of options for adaptive scanning for forecasters, ostensibly each with different usage patterns and levels of success in contributing to skillful severe weather warning issuance. This study aims to address the following questions:

- What is the breakdown of VCP selection near NWS warnings and storm reports and have these VCP selections evolved over the last decade?
- How often was a SAILS strategy used for storms that had NWS warnings issued and/or an associated storm report?
- Do more rapid low-level supplemental scans improve warning performance?
- How do forecasts for organized thunderstorms, such as the issuance of severe thunderstorm and tornado watches by the Storm Prediction Center, influence the selection of SAILS strategies?
- How have radar volume update times around tornado, hail, and thunderstorm reports changed over the past decade?

Section 2 describes the data and methods, section 3 summarizes how VCPs and supplemental scanning strategies have been used over the last decade, and section 4 covers a discussion and summary of findings.

2. Data and methods

a. Warning dataset development

All severe thunderstorm and tornado warnings from 2011 to 2020 were downloaded from the NWS Performance

Management web page.[1] For each warning, the product text was parsed to get the warning location (from the LAT…LON line) and the warning tracking point (from the TIME…MOT…LOC line). The tracking point was used to determine which WSR-88D radar was closest to the warning, and the issuance time was used to determine the time window of data to request. Other warning metadata included whether the warning was verified by a severe weather report. This information was combined with the VCP information to determine how warning performance scores change with different supplemental intra-volume scanning strategies. The initial NWS warning dataset used for analysis included 189 107 severe thunderstorm warnings and 24 928 tornado warnings.

b. Storm report dataset development

All severe weather reports (thunderstorm wind, hail, and tornado) from 2011 to 2020 were downloaded from the NWS Performance Management *Storm Data* report archive. *Storm Data* is a comprehensive listing of all *reported* severe thunderstorm hazards and is commonly used as ground truth to examine radar signatures (e.g., Stumpf et al. 1998) and hazard impacts (e.g., Black and Ashley 2011). This archive is susceptible to a number of errors in report time, location, or other metadata and can underrepresent a significant event due to lack of reports (Witt et al. 1998b; Trapp et al. 2006; Ortega et al. 2009). In a large climatological analysis such as the one herein, the extent of these errors should have a negligible impact on the resulting trends observed. For each severe weather report, the reported start location and time were used to determine the closest radar and time window to download. The metadata also contains the magnitude of the storm report (i.e., hail size, wind speed, tornado rating). As with warning information, storm report data were combined with the closest radar VCP information to break down how higher versus lower impact events are scanned by the WSR-88D.

Currently, NWS severe thunderstorm warnings are verified by a thunderstorm wind gust equal to or exceeding 50 kt (58 mph; 1 kt ≈ 0.51 m s^{-1}) or a hail size of 1-in. diameter or greater (NWS 2020). There were 26 136 hail and 5 204 wind reports from 2011 to 2020 that did not meet these criteria and were removed. The resulting storm report database used for analysis included 13 488 tornado reports, 77 865 hail reports, and 159 547 wind reports.

c. Level-II radar dataset development

For each warning and report, WSR-88D Level-II data from ±30 min around each warning or report start time were downloaded from the archive hosted on Amazon Web Services[2] (AWS; Ansari et al. 2018). To ensure the most complete possible dataset was used for this study, files unavailable on AWS were manually requested for download via the NOAA National Centers for Environmental Information (NCEI) Level-II historical archive web page.[3] Each downloaded Level-II file was read into the Python ARM Radar Toolkit (Py-ART; Helmus and Collis 2016) to retrieve the VCP number, elevation angles, and elevation angle times.

SAILS, MESO-SAILS, MRLE, and AVSET are not directly reported within the radar metadata like the VCP number. These strategies were determined by examining the elevation angles in the radar volume. A volume scan with one, two, or three extra low-level (usually 0.5°) scans was classified as SAILSx1, SAILSx2, and SAILSx3, respectively. For MRLE, a volume scan with an extra 0.5°/0.9° was reported as MRLEx2, an extra 0.5°/0.9°/1.3° as MRLEx3, and an extra 0.5°/0.9°/1.3°/1.8° as MRLEx4.

After processing the radar data, entries in the warning or storm report analysis dataset were removed if either 1) the WSR-88D data were missing or the archived Level-II files were unreadable with ±30 min of the event or 2) the closest WSR-88D did not have dual-polarization capabilities yet. From the accessible NEXRAD archive, 97.2% (n = 183 572) of severe thunderstorm warnings, 96.2% (n = 23 973) of tornado warnings, 96.4% (n = 12 992) of tornado reports, 97.7% (n = 76 093) of hail reports, and 97% (n = 154 742) of wind reports had available data from the closest WSR-88D from 2011 to 2020. The first dual-polarization upgrade to a WSR-88D in the continental United States occurred with the Vance Air Force Base (KVNX) site in northwest Oklahoma on 8 March 2011 and the final upgrade was completed on the Moody Air Force Base (KVAX) site in southern Georgia on 16 May 2013 with all other sites scheduled in-between. In 2011, 20 sites were upgraded with dual-polarization capabilities, 98 sites were upgraded in 2012, and the remaining 25 were completed in 2013. Discarding all nonpolarimetric warnings and events brings the final number of cases analyzed to 148 882 severe thunderstorm warnings, 18 263 tornado warnings, 10 474 tornado reports, 58 934 hail reports, and 127 575 wind reports.

Given that outbreak events can have multiple warnings or storm reports in close space or time proximity to a single radar, a subset of this full dataset was sampled by taking the first warning and removing all subsequent warnings of that type that occurred within the next 30 min near that radar site. For storm reports, the warning time rules were used, but the highest magnitude report (i.e., largest hail size) was returned for that 30-min window. This will limit the influence of outbreaks or other high-impact events from skewing the summary statistics. Results from this restricted dataset will be reported as the "subset" of warnings and storm reports. The number of elements analyzed in the "subset" include 91 986 severe thunderstorm warnings, 11 641 tornado warnings, 6254 tornado reports, 28 474 hail reports, and 51 246 wind reports. Unless otherwise stated, all results discussed below are referencing the entire climatology of warnings or storm reports rather than this subset.

d. Warning verification

Since the transition to storm-based warnings on 1 October 2007, the NWS determines its convective warning performance using either a generic or event-specific verification system (NWS 2009). In the generic system, any severe hazard (hail ≥ 1 in., wind ≥ 50 kt, or a tornado) verifies either a severe thunderstorm warning or a tornado warning. In the

[1] https://verification.nws.noaa.gov/.
[2] https://registry.opendata.aws/noaa-nexrad/.
[3] https://www.ncei.noaa.gov/has/HAS.DsSelect.

event-specific verification system, a hail or wind report can only verify a severe thunderstorm warning and only a tornado report can verify a tornado warning. This study adopts a modified version of the event-specific warning system with special handling of the scenario where wind and hail events occur inside tornado warnings. In that scenario today, the hail/wind event would count as being inside a warning (i.e., a hit) but the tornado warning itself would not be verified by that event (i.e., a false alarm). This study focuses on the analysis of the primary hazards expected by the warning type so as to not artificially inflate the skill in predicting the occurrence of hail and wind hazards. We exclude all instances where wind and hail reports occur inside tornado warnings before calculating the probability of detection (POD) for the storm reports and false alarm ratio (FAR) for the convective warnings. A similar verification approach was performed in Wilson et al. (2017) to highlight that forecasters were making the correct warning decision appropriate for the anticipated hazard. To provide an estimate of the distribution of POD and FAR with a SAILS or MRLE strategy, the events and warnings matching that strategy were resampled at 50 000 iterations using a nonparametric ordinary bootstrap technique (Efron 1979) to develop a 99% confidence interval. To determine whether a SAILS or MRLE strategy with more low-level scans resulted in a statistically significantly higher POD and lower FAR, the bootstrapped samples were compared using a one-sided nonparametric Mann–Whitney U test (Mann and Whitney 1947).

e. *Spatiotemporal comparison with Storm Prediction Center watches*

The NWS Storm Prediction Center (SPC) should issue a severe thunderstorm watch if there is a forecast of six or more 1+-in. hail or 50+-kt wind events over at least an 8000-mi^2 area and 2-h time period. A tornado watch should be issued if there are organized thunderstorms forecast to produce two or more tornadoes or any tornado which could produce EF2+ damage (NWS 2021). These watches are typically issued several hours in advance of a convective event and are coordinated with the potentially affected offices before issuance. Given these watches represent a region and time with an increased risk of severe convective activity, the location and time information from warnings and events in this study was used to determine if it was inside a severe thunderstorm or tornado watch. The SPC watch information was collected from the SPC website[4] and the Universal Geographic Code was used to determine the counties inside each watch. In total, 3778 severe thunderstorm and 1718 tornado watches from 2011 to 2020 were examined.

f. *Quantifying the loss of upper-atmosphere observations*

To quantify the impact of SAILS on detecting mid- to upper-atmosphere features, we examined which elevation angle intersects 1 km above the height of the 0°C isothermal level for the warning tracking point or storm report. This height level is commonly used for Z_{DR} column detection (e.g., Van Den Broeke 2017; French and Kingfield 2021). This height also provides sufficient distance away from the 0°C isothermal level as the local 0°C level can be perturbed upward from vertical advection and latent heating effects within a convective updraft (Snyder et al. 2015). The 0°C isothermal level was collected from the 13-km Rapid Refresh (RAP; Benjamin et al. 2016) using the Warning Decision Support System-Integrated Information (WDSS-II; Lakshmanan et al. 2007) software and the height of the WSR-88D beam from the closest radar was calculated for each warning and storm report. If RAP data were unavailable for a storm report or warning then it was excluded from this part of the analysis.

3. Results

a. *VCP selection near NWS warnings and storm reports*

Over the study period there was a decline in selectable VCPs for tracking precipitation systems. From 2011 to 2018, there were seven VCPs available for this purpose. VCP 12 and 212 (Fig. 1a) provided more dense low-level sampling of the atmosphere during severe weather, VCP 11 and 211 for better sampling aloft, VCP 21 and 221 for improved data quality, and VCP 121 for observing tropical systems and widespread precipitation events (ROC 2015). VCPs 211, 212, and 221 scan at the same angles as VCPs 11, 12, and 21 but implement an improved algorithm for range folding mitigation in velocity data with the use of the second version of the Sachidananda and Zrnić (SZ-2; Sachidananda and Zrnić 1999) systemic phase code for resolving range overlaid signals. In 2018, VCP 215 was introduced to provide a general surveillance VCP that contains the best features of VCPs 211, 212, and 221 (Fig. 1b) and VCPs 11, 211, 21, and 221 were retired, leaving four selectable precipitation VCPs. In 2020, VCP 112 was released to replace VCP 121; it provides back-to-back velocity scans at different pulse repetition frequencies for enhanced low-level velocity interrogation (Zittel 2019).

1) NWS SEVERE THUNDERSTORM AND TORNADO WARNINGS

In NWS convective warning operations, forecasters strongly preferred using a VCP that provides dense sampling coverage at lower levels of the atmosphere. A large majority of severe thunderstorm (86%–97.5%) and tornado warnings (89.5%–100%) had the closest radar scanning in VCP 12/212 in any single year (Fig. 2). Other VCPs that highlight better sampling at midlevels and improved data quality were used around 8%–16% of the time in 2011 and 2012 and declined to around 1% of all warnings by 2018. As expected, for each year, a higher ratio of tornado warnings were near a radar scanning in VCP 212 over VCP 12 compared to severe thunderstorm warnings, ostensibly to take advantage of the output from the SZ-2 velocity algorithm. While beneficial for velocity interpretation, it takes around 21 s longer to process a volume of information in VCP 212 compared to VCP 12. Since the beginning of the dual-polarization era, 94% (3%) of severe

[4] https://www.spc.noaa.gov/.

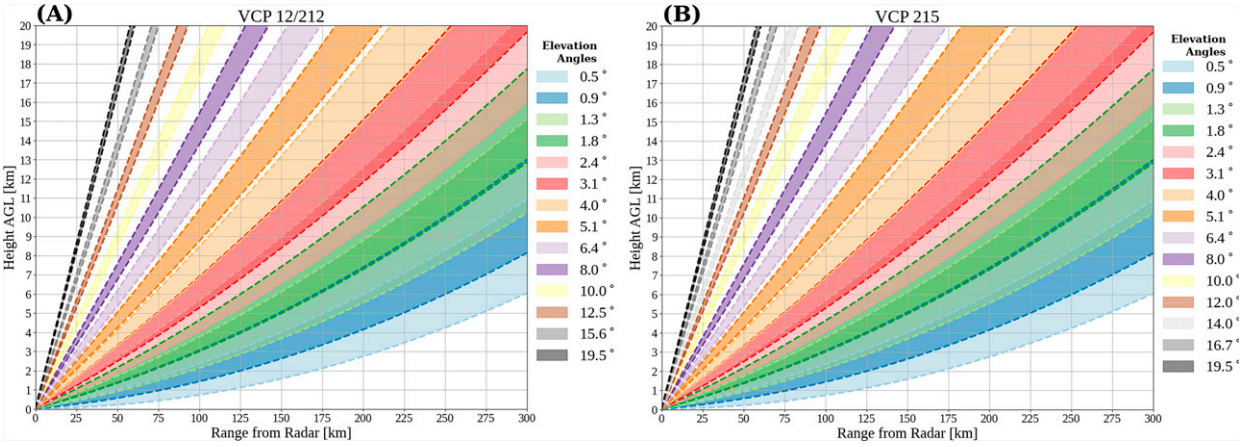

FIG. 1. Elevation angles scanned by a WSR-88D in (a) VCP 12/212 and (b) VCP 215. The dashed lines correspond to the bottom and top of the beam as it moves away from the radar. Both VCPs are similar below 10° with VCP 215 providing more closely spaced scans above 10° when compared to VCP 12/212.

thunderstorm warnings and 96% (1.9%) of tornado warnings had its closest radar scanning in VCP 12/212 (215). Similar trends are seen with the data subset that removes multiple warnings occurring within 30 min of the initial warning near the same radar.

2) STORM REPORTS

Consistent with the strong preference to maximize low-level sampling coverage during NWS warning operations, most convective hazards were also scanned using these same VCPs. A large majority (≥89%) of tornado, hail, and wind reports had their closest radar scanning with VCP 12 or 212 in any single year (Figs. 3a–c). This trend is also observed when the full dataset is subset to discard multiple reports that occur within 30 min of an initial report (≥85%). The usage of other VCPs was greater in earlier years, particularly near thunderstorm wind reports (10%–14%). With time, the adoption of these VCPs declined to around 5% by 2014 and around 1% by 2018 when they were retired. In 2018, VCP 215 became the third most used VCP with around 4%–10% usage depending on the report and dataset types.

Since the beginning of the polarimetric data era, 95.9% (1.8%) of tornado reports, 95.3% (2%) of hail reports, and 95% (2.4%) of wind reports had its closest radar scanning in VCP 12/212 (215). The results are similar for

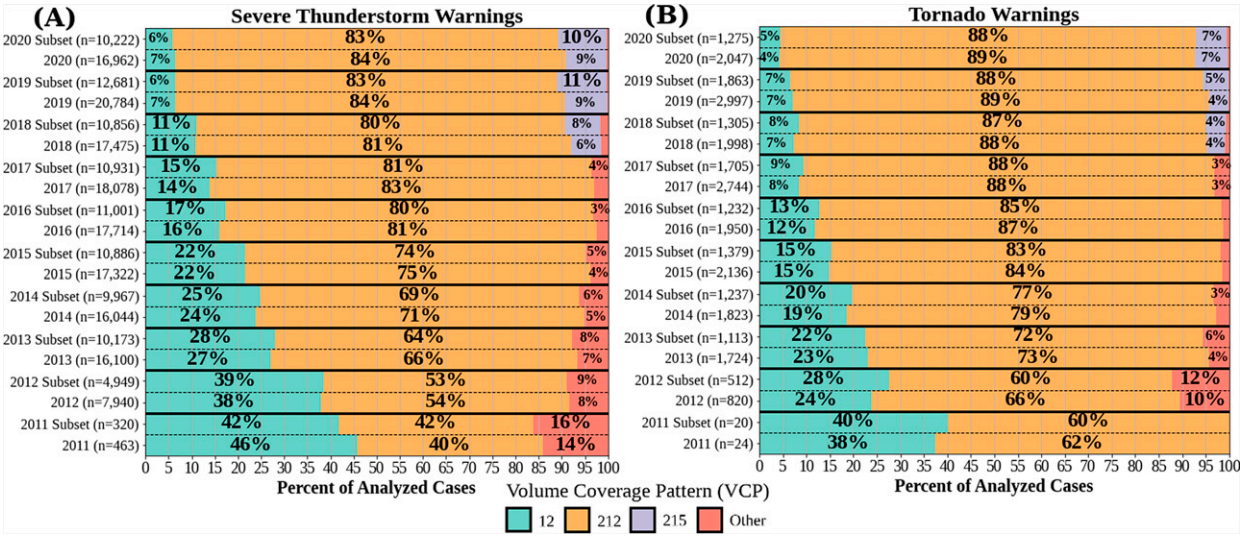

FIG. 2. Yearly percentage of VCPs used by the nearest radar to (a) severe thunderstorm and (b) tornado warnings. Each year is presented for all warnings near a dual-polarization radar and a subset that eliminates multiple warnings of the same type occurring within 30 min near the same radar site.

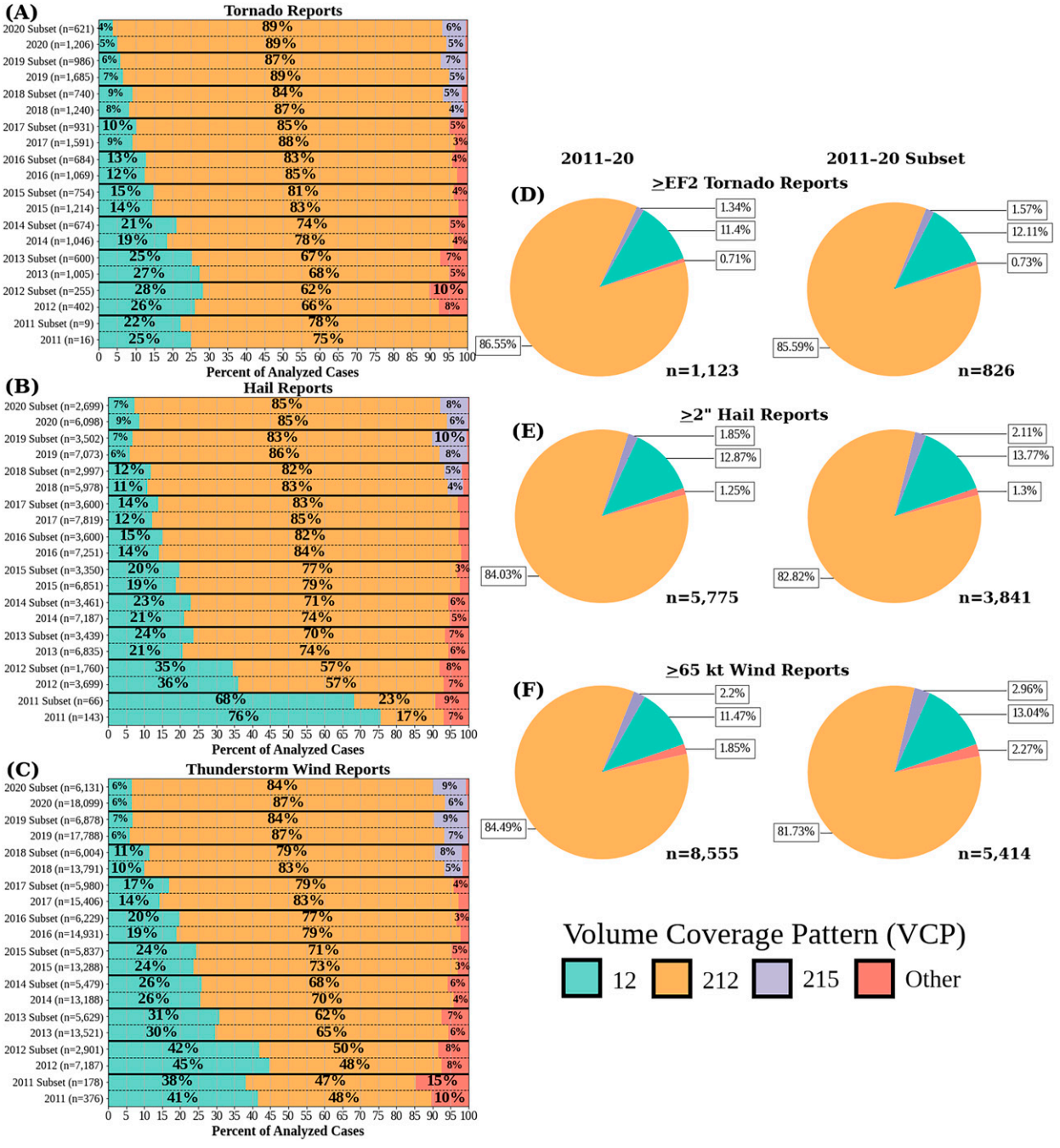

FIG. 3. Yearly percentage of VCPs used by the nearest radar to (a) tornado, (b) hail, and (c) thunderstorm wind reports. Each year is presented as all reports near a dual-polarization radar and a subset that eliminates multiple warnings of the same type occurring within 30 min near the same radar site. The pie charts on the right show the VCP breakdown near storm reports of significant (d) tornadoes (EF2+), (e) hail (≥2 in.), and (f) thunderstorm winds (≥65 kt).

significant severe events (Figs. 3d–f): 98% (0.7%) of tornado reports rated EF2 or stronger, 96.9% (1.3%) of hail reports exceeding 2 in. in diameter, and 96% (1.9%) of wind reports exceeding 65 kt had its closest radar running with VCP 12/212 (215). *VCPs 12, 212, and 215 employ the same sampling strategy below 10° above the radar horizon, resulting in the lowest 1 km of the atmosphere being sampled the same way for all convective hazards*. Since nearly all convective hazards in the polarimetric data era are scanned using these VCPs, there is a climatological consistency in how low-level thunderstorm features are actively measured by the radar.

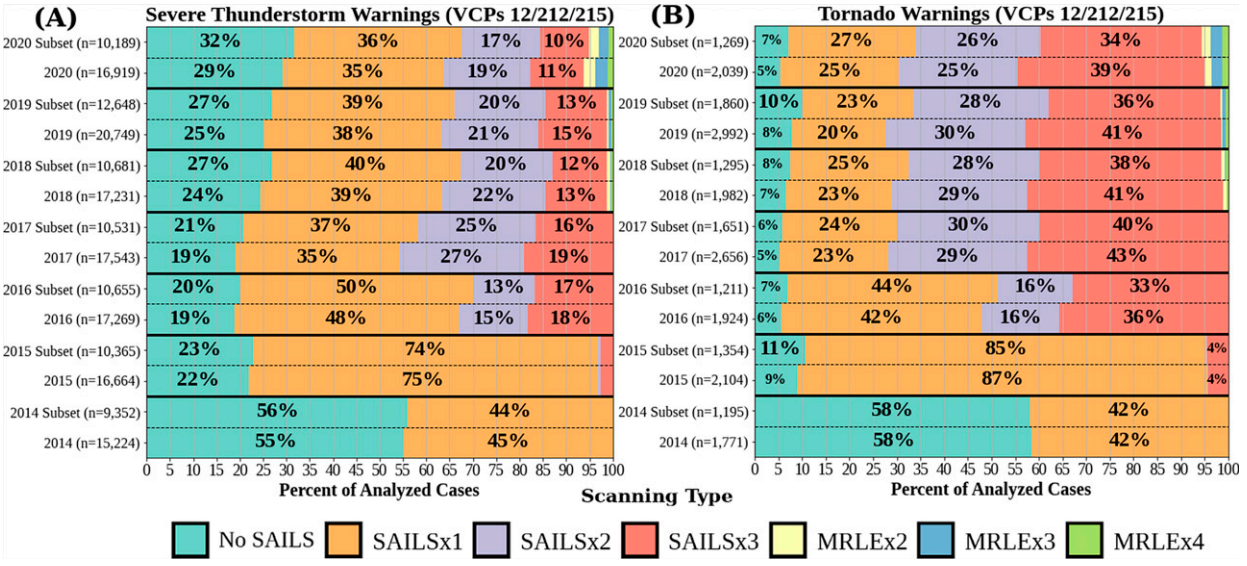

FIG. 4. Yearly percentage of SAILS and MRLE selections for (a) severe thunderstorm warnings and (b) tornado warnings. Each year is presented as all warnings near a dual-polarization radar and a subset that eliminates multiple warnings of the same type occurring within 30 min near the same radar site.

b. Supplemental low-level strategy selection near NWS warnings and reports

Since 2014, there have been three precipitation-focused VCPs that allow for supplemental low-level angles. VCPs 12 and 212 had the option to select SAILSx1 in 2014, SAILSx2 and SAILSx3 in 2015, and MRLEx2-x4 in 2018. Since the creation of VCP 215, forecasters have had the ability to use either SAILSx1 or MRLEx2-x4. VCPs 11, 211, 21, and 221 were never updated to use any of these strategies until their deactivation. This subsection will focus on the VCPs that allow for supplemental low-level scans. As noted in section 3a, these three VCPs were used near 97.3% of the storm reports, 96.9% of the severe thunderstorm warnings, and 97.8% of the tornado warnings in the study.

1) NWS WARNINGS

The option to add supplemental low-level scans to a radar volume was rapidly adopted in NWS warning operations after the initial national implementation of SAILS. Since 2015, SAILS strategies have been activated during a majority of warning decision-making moments for both severe thunderstorm and tornado warnings. Over 70% of severe thunderstorm and 89.7% of tornado warning decisions were made with the closest radar to the storm scanning with a SAILS strategy activated in any single year (Fig. 4). Since the first full year of MESO-SAILS in 2016, 75.5% of severe thunderstorm warnings and 92.6% of tornado warnings had SAILS or MRLE activated. For severe thunderstorm warnings, SAILS strategies with fewer supplemental angles were more widely used. SAILSx1, SAILSx2, and SAILSx3 were in use nearby 38.4%, 20.3%, and 15.1% of warnings, respectively. For tornado warnings, SAILS strategies with more supplemental angles were commonly used. 39.8% of all warning decisions were made with the closest radar in SAILSx3, followed by 26% with SAILSx2 and 25.3% with SAILSx1.

Since the beginning of the polarimetric data era, 40.5% (25.9%) of severe thunderstorm (tornado) warning decisions were made without any SAILS or MRLE running at the nearest radar and most of these warnings occurred between 2011 and 2014 when no SAILS strategies existed. Breaking down the overall SAILS activation types over this last decade, 36.4% (30.3%) of severe thunderstorm (tornado) warned storms had its closest radar in SAILSx1, 12.5% (16.7%) in SAILSx2, 9.5% (26.1%) in SAILSx3, and 1% (0.9%) in MRLEx2/MRLEx3/MRLEx4. Given this trend, it is expected that SAILS and MRLE will continue to be active in a vast majority of warned storms for the foreseeable future.

2) STORM REPORTS

There has been a notable increase in the number of low-level scans since the nationwide activation of SAILS in 2014–15 (Figs. 5a–c). Since 2015, the closest radar has been scanning with extra low-level scans activated for 90%–92.8% of tornadoes, 73.1%–81.4% of hail events, and 77.2%–82.1% of wind reports in any single year (Figs. 5a–c). The addition of SAILSx2 and SAILSx3 in 2016 resulted in 52.6%–70.7% of tornado events in any given year since 2016 being scanned with more than one extra low-level scan. As expected given the limited usage of SAILSx2 and SAILSx3 when severe thunderstorm warnings are issued, these SAILS strategies are used less frequently for hail and wind reports with 29.6%–49.8% and 31.3%–51.7% of the reported hazards using this scan in any given year from 2016 to 2020.

Since the beginning of the polarimetric data era through the end of 2020, around 74.7% of all tornado reports, 58.8% of hail reports, and 62.7% of wind reports were scanned with

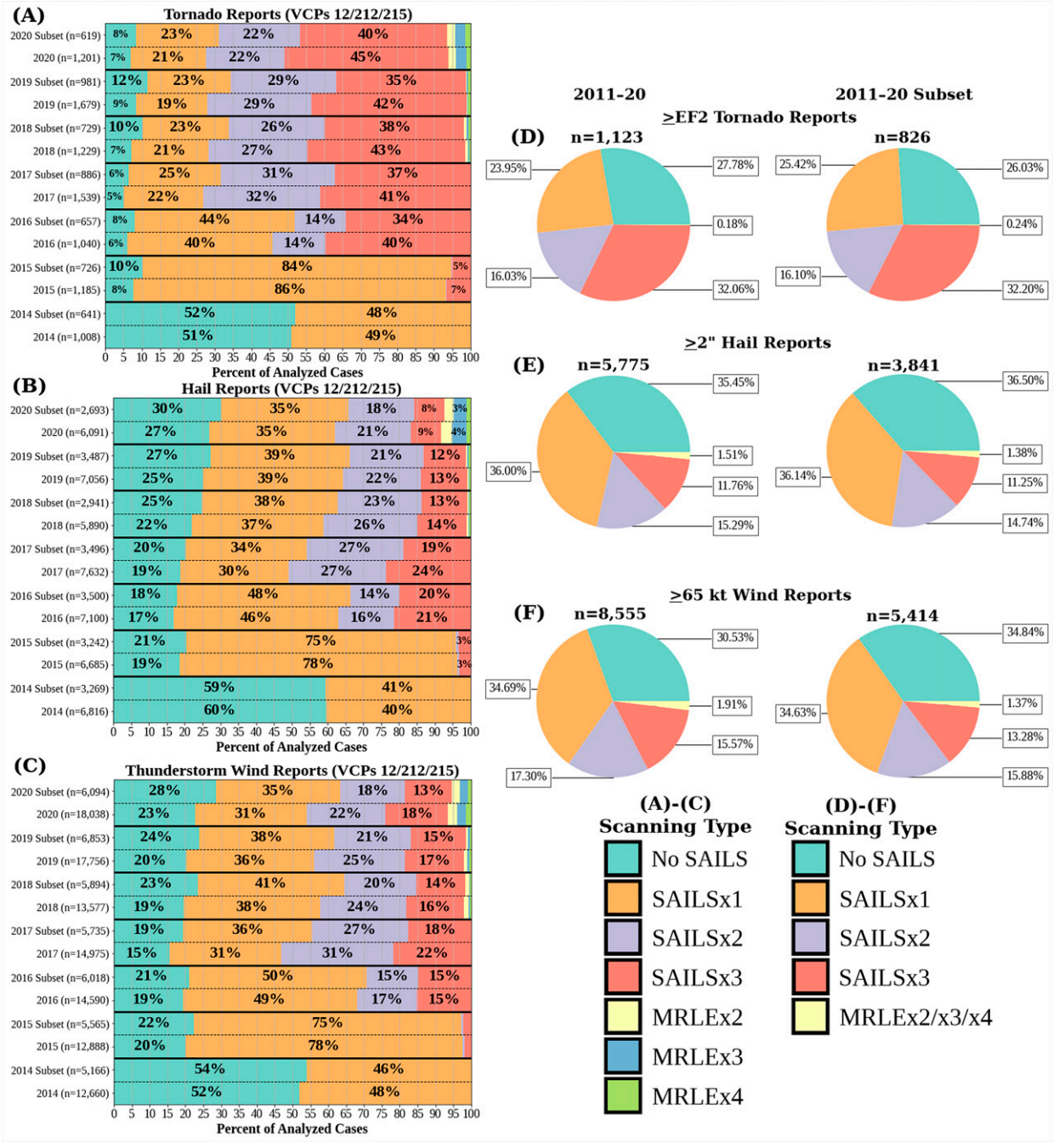

FIG. 5. Yearly percentage of SAILS and MRLE selections for (a) tornado, (b), hail, and (c) wind reports. Cumulative percentage of significant severe hazards scanned with SAILS, MESO-SAILS, and MRLE selections for (d) tornado, (e) hail, and (f) wind reports (left) from 2011 to 2020 and (right) via the subset method to remove multiple reports within 30 min each other at the same radar and retain the strongest report.

the closest radar adding additional low-level angles. Around 29.5% of all tornadoes were scanned with SAILSx1, 16.4% with SAILSx2, 27.7% with SAILSx3, and around 1.1% with a MRLE strategy. For hail reports, the closest radar is using SAILSx1, SAILSx2, SAILSx3, and MRLE 35%, 12.9%, 9.8%, and 1% of the time, respectively. For all wind reports, these strategies are used 35.4%, 14.9%, 11%, and 1.4% of the time. For significant severe hazards, 72.2% of EF2+ tornadoes, 64.6% of hail reports exceeding 2 in., and 69.5% of wind reports exceeding 65 kt were scanned by a radar with extra low-level angles (Figs. 5d–f). Similar trends are found after removing duplicate reports of the same type. The percentage

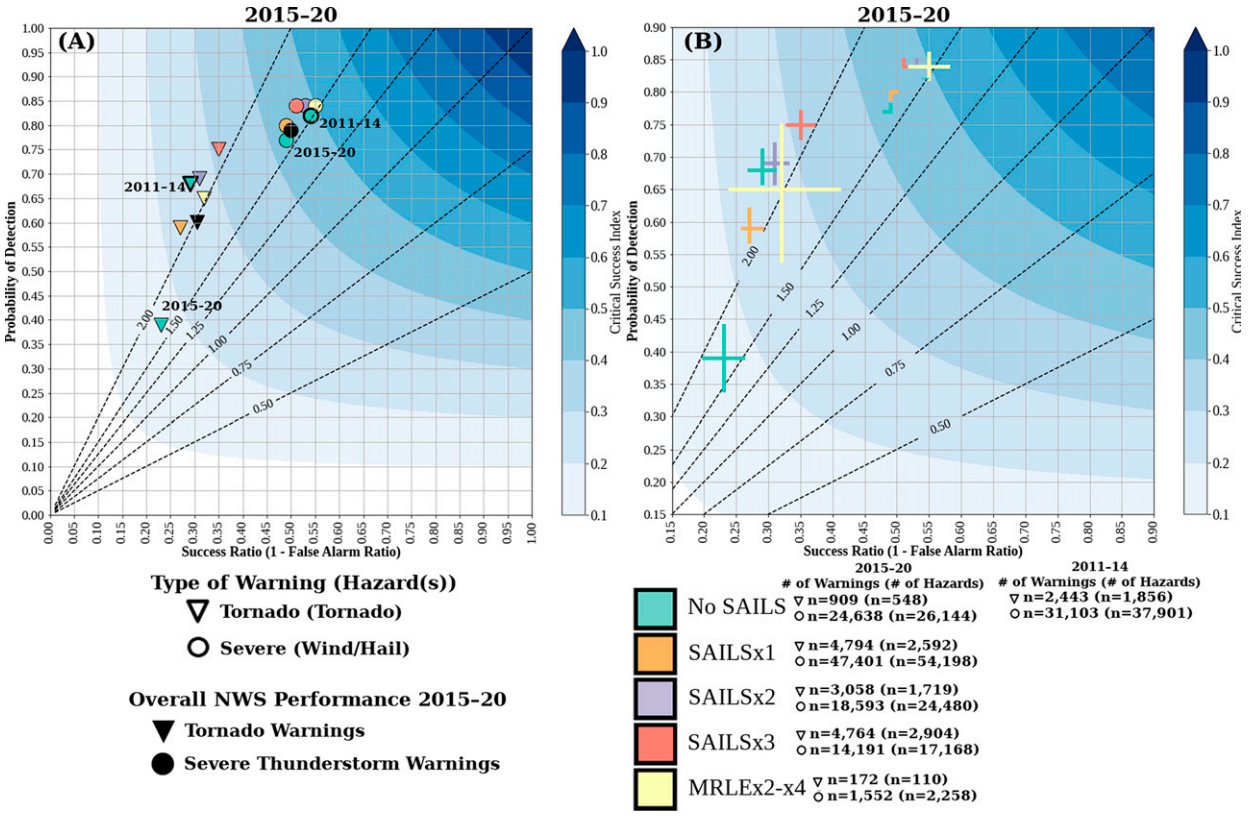

FIG. 6. Receiver operating characteristic curve showing (a) warning performance for severe thunderstorm and tornado warnings/hazards by SAILS or MRLE type and (b) the 99% confidence interval of warning performance by SAILS or MRLE type from 2015 to 2020. The performance of the No SAILS category was also plotted (with a larger black outline) from 2011 to 2014 to highlight the decline in usage and performance once other SAILS strategies were available.

of significant severe reports scanned with a SAILS strategy is 74%, 63.5%, and 65.1% of tornado, hail, and wind reports, respectively.

c. *NWS warning performance by supplemental low-level strategy selection*

Separating the warning decisions and associated hazards by supplemental low-level strategy used reveals an overall range of POD (FAR) of around 0.07 (0.06) for severe thunderstorm warnings and a 0.36 (0.08) for tornado warnings (Fig. 6). For severe thunderstorm warnings, MRLEx2-x4 had the same POD (0.84) as SAILSx2 and SAILSx3 with a slightly lower FAR of 0.45 compared to 0.47 and 0.49, respectively. One suspected reason for this is that it is a best practice for MRLE to be used when scanning QLCS convective modes to diagnose quick tornado "spinups." Furthermore, this mode can produce severe hail mainly during its initial developmental stage and more widespread severe winds in its mature stage resulting in a large quantity of storm reports (Smith et al. 2012). Using SAILSx2 and SAILSx3 showed a statistically significantly higher POD and lower FAR than SAILSx1 or No SAILS, but cases where SAILSx3 was used were not statistically significantly better performance-wise than SAILSx2. Examining POD and FAR by year (Figs. 7a,c) reveals an increase in POD for warnings issued with SAILSx2/x3 over time and a nearly stationary POD for SAILSx1 and No SAILS. A higher percentage of severe thunderstorm warnings issued with SAILSx2/x3 verified compared to warnings issued near radars with slower revisit speeds at lower angles, particularly during 2017–20. Given the nearly equal warning and event detection performance between SAILSx2 and SAILSx3, *SAILSx2 may be a preferred choice to gain more frequent updates at higher elevation angles during severe thunderstorm warning operations.*

Tornado warnings issued with the closest radar producing more low-level scans had higher POD and lower FAR performance metrics. SAILSx3 had the highest POD and lowest FAR (0.75/0.65) while using No SAILS had the lowest POD and highest FAR (0.39/0.77) from 2015 to 2020. Comparing the No SAILS statistics from 2015–20 to 2011–14, there has been a prominent decline in the number of tornado warnings issued, a decline in POD by 0.26 and an increase in FAR by 0.06. Tornado warnings issued with SAILSx3 activated had a statistically significantly higher POD and lower FAR when compared against all other SAILS/No SAILS strategies. SAILSx2 also provided a statistically significant performance improvement over SAILSx1 or No SAILS activated. Over the

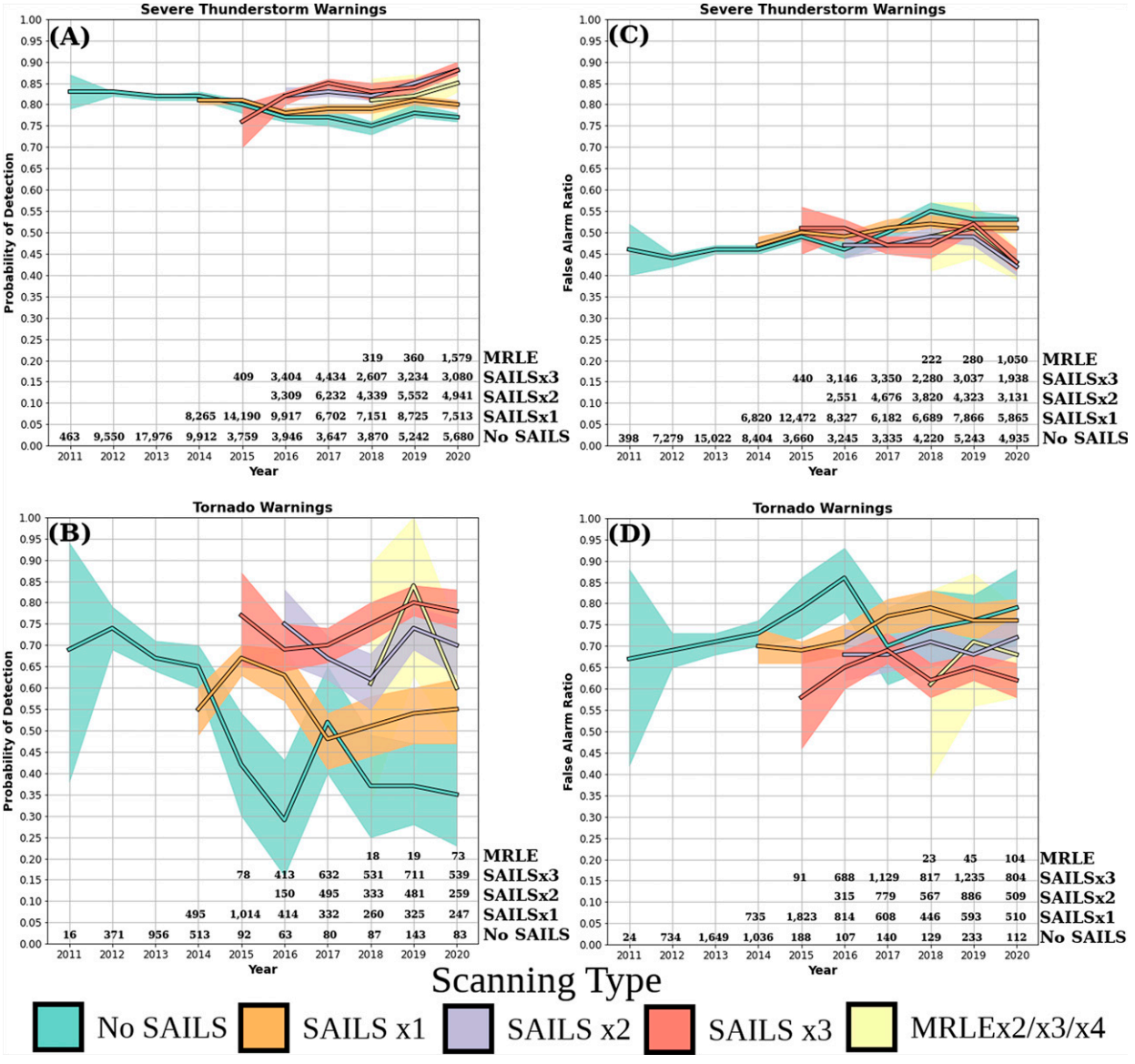

FIG. 7. Yearly performance metrics with probability of detection (POD) for (a) severe thunderstorm and (b) tornado warnings and false alarm ratio (FAR) for (c) severe thunderstorm and (d) tornado warnings by supplemental low-level scanning strategy. The shaded area represents the 99% confidence interval calculated using a nonparametric ordinary bootstrap resampling technique. There was one unverified SAILSx2 tornado warning issued in 2015, resulting in a POD of 0 and a FAR of 1. This data point was excluded from the time series above.

years, SAILSx2/x3 consistently had a higher POD and lower FAR than the SAILSx1 or No SAILS categories (Figs. 7b,d).

The improvements in POD and FAR using SAILS also translate into better lead times for specific hazards (Fig. 8). Of the 456 tornado reports near a radar with the No SAILS strategy, only 35.7% had a tornado warning issued with a positive lead time. *Tornado lead times improve with a greater number of supplemental low-level scans: 53.4% (n = 1,578), 67.5% (n = 1718), and 73.5% (n = 2826) of tornado reports had a tornado warning with positive lead time using SAILSx1, SAILSx2, and SAILSx3, respectively.* Similar trends were observed for wind hazards with 71.7% (84.4%) of events having a positive warning lead time with No SAILS (SAILSx3) strategy selected. SAILSx2 and SAILSx3 had nearly equal positive lead times for 88.7% of hail events and it is an improvement over the No SAILS events where 84.6% of events had a positive lead time.

d. *Supplemental low-level strategy selection inside Storm Prediction Center watches*

From 2011 to 2020, 39.4% (n = 56 971) of severe thunderstorm warnings and 66.6% (n = 11 907) of tornado warnings

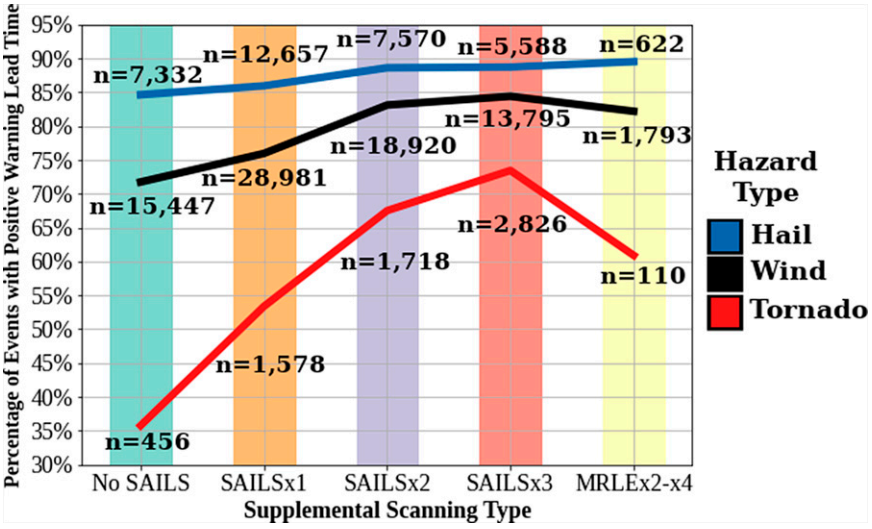

FIG. 8. Percentage of hazards that were warned with a positive lead time by supplemental low-level scanning strategy. The sample size of each hazard is annotated.

were issued inside an SPC watch area (Fig. 9). For severe thunderstorm warnings, 27.3% (n = 39 403) were in a severe thunderstorm watch and 12.2% (n = 17 568) were in a tornado watch. For tornado warnings, 17.5% (n = 3130) were inside a severe thunderstorm watch and 49.1% (n = 8777) were inside a tornado watch.

Examining tornado watches from 2016 to 2020, when SAILSx1–x3 were fully available, SAILSx3 was the dominant supplemental scanning strategy used during tornado watch operations. SAILSx3 supported the issuance of 39.5% (n = 3973) and 47.9% (n = 2618) of all severe thunderstorm (n = 10 044) and tornado (n = 5470) warnings inside tornado watches. SAILSx2 was the second most frequently used strategy, supporting the issuance of 27.6% (n = 2775) and 25.9% (n = 1420) severe thunderstorm and tornado warnings inside tornado watches. Overall, 93% (95%) of severe thunderstorm (tornado) warnings issued inside a tornado watch used a SAILS strategy.

During severe thunderstorm watch operations from 2016 to 2020, the closest radar was running SAILSx3 15.5% (n = 3817) of the time and was the least used of the SAILS strategies when issuing severe thunderstorm warnings. SAILSx1 (38.3%; n = 9442) and SAILSx2 (24.6%; n = 6045) were used more frequently in issuing severe thunderstorm warnings over this period. For tornado warnings, SAILSx1-SAILSx3 strategies were used in around 87% of the warnings issued. SAILSx2, SAILSx1, and SAILSx3 supported 30.9% (n = 648), 29.2% (n = 612), and 26.9% (n = 564) of tornado warnings inside severe thunderstorm watches, respectively.

Overall, 75.2% (n = 15 789) and 48.3% (n = 348) of severe thunderstorm and tornado warnings issued with no supplemental low-level scanning strategy were issued outside of an SPC watch. In comparison, 43.3% (n = 5961) and 31.9% (n = 1461) of severe thunderstorm and tornado warnings issued with the support of a SAILSx3 scan occurred outside of an SPC watch. This suggests that SAILS strategies are used more frequently in environments more conducive to producing convective hazards and verifying warnings, and could explain some of the increase in POD and decrease in FAR summarized in section 3c.

Organizing the warnings by the presence of a SPC watch reveals that when no watch is issued, a greater percentage of severe thunderstorm and tornado warnings issued with the closest radar running SAILSx2 or SAILSx3 were verified by a storm report (Fig. 10). When a severe thunderstorm watch was issued, severe thunderstorm warnings with the closest radar running SAILSx2 had the highest verification percentage, and it was statistically significantly higher ($p < 0.01$) than warnings issued with SAILSx1 or No SAILS. SAILSx3 was the least used strategy and had a slightly worse verification percentage than SAILSx1. Inside tornado watches, severe thunderstorm warnings with SAILSx2 and SAILSx3 outperformed SAILSx1 and No SAILS and these verification scores were statistically significantly higher than the strategies with one or no additional low-level elevation angle. For tornado warnings, SAILSx3 warnings performed the best regardless of SPC watch type and the resampled distribution of verification percentages were statistically significantly better than SAILSx2, SAILSx1, and No SAILS.

e. Impacts of using supplemental strategies on upper-atmosphere observations

The widespread adoption of adding supplemental low-level scanning strategies to a standard volume of data is almost certainly beneficial for diagnosing low-level features seen by the lowest elevation angle. But the cost of employing the additional low-level scans is a longer delay between scans used for examining features aloft. For example, the Z_{DR} column region, defined here as 1 km above the height of the 0°C isothermal level, is observed by an elevation angle greater than 0.5° in 99.3% of all convective storm reports evaluated (n = 189 206) (Fig. 11). The selection of any SAILS strategy will increase the time between these higher scans by 31–93 s for

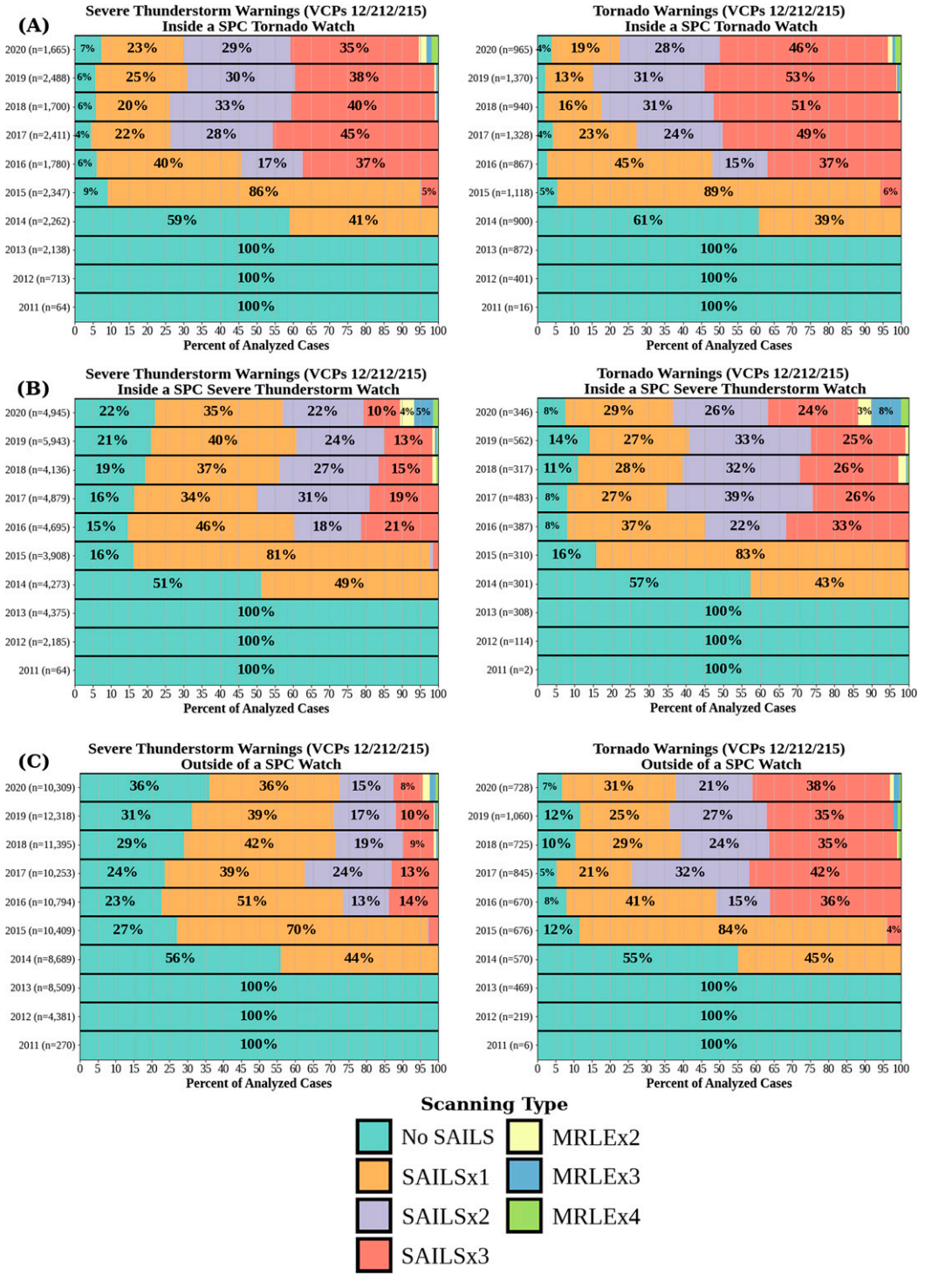

FIG. 9. Yearly percentage of SAILS, MESO-SAILS (SAILSx2, SAILSx3), and MRLE selections in conjunction with (left) severe thunderstorm warnings and (right) tornado warnings inside (a) tornado watches, (b) severe thunderstorm watches, and (c) no watch issued by the SPC.

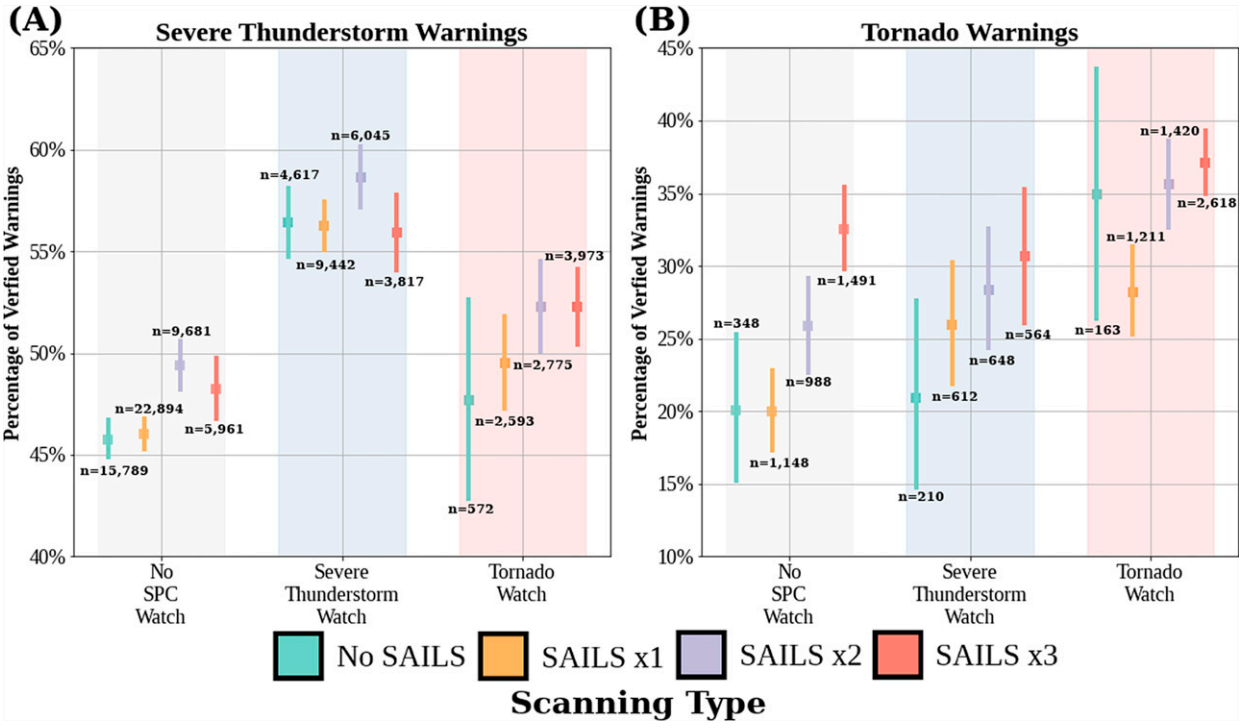

FIG. 10. Warning verification percentage for (a) severe thunderstorm warnings and (b) tornado warnings outside of an SPC watch, inside a severe thunderstorm watch, and inside a tornado watch. The vertical lines correspond to the 99% confidence interval constructed by resampling the warnings with replacement through 50 000 iterations.

VCP 12, 38–114 s for VCP 212, and 53 s for VCP 215. The adoption of MRLEx2 through MRLEx4 could provide extra scans of the Z_{DR} column in 3.2%, 9.9%, and 22.7% of potential cases, respectively; however, a MRLE strategy has been used in only around 1% of cases to date. Within 50 km of a radar, the Z_{DR} column was best visible at an elevation angle 2.4° or higher and there are no supplemental scanning strategies with extra scans at these angles. If a column were to exist at 2.4° or higher, the usage of MRLEx2 through MRLEx4 with VCP 215 would increase the time between similar scans at or above 2.4° by 100, 144, and 169 s, respectively. Selecting MRLEx2 exceeds the maximum SAILSx3 time increase for VCP 12 and the SAILSx2 time increase for VCP 212, resulting in even slower revisit times for higher angles. Even though the Z_{DR} column region is being described here, these numbers can apply to many other convective features measured above the 0.5° elevation angle and the revisit times to these regions is increasing.

There has been a notable decline in volume update frequency since the national implementation of these supplemental scanning strategies (Fig. 12). From 2011 to 2013, over 16% of tornado reports, 20% of hail reports, and 16% of wind reports were being scanned at a faster rate than the standard VCP 12/212 volume time due to early volume termination with AVSET activated. Starting in 2014, volume update times in around 46% of tornado reports, 37% of hail reports, and 45% of wind reports were slower than the standard VCP 12/212 volume time. By 2015, a single radar volume was taking 15% longer to complete near 60% of tornado reports, and around 47% of hail and wind reports. These volume update speeds are even slower for a majority of cases in recent years. From 2016 to 2020, 25%–35% of WSR-88Ds scanning tornadoes were taking 45% longer to complete a single volume of data. For elevation angles with no options for extra scans (i.e., 2.4° or higher), the revisit time for these regions of the atmosphere slows down from around 4.5 min to around 6.5 min. This results in around four fewer scans at these regions per hour.

These extra low-level angles also diminish the effectiveness of AVSET as it takes longer to scan the lowest levels of the atmosphere. Since 2016, radar volumes for around 5% of tornado reports, 10%–15% of hail reports, and 10% of wind reports were being produced at a faster speed than the standard volume time. In any single year since 2016, over 89% of tornado reports, 69% of hail reports, and 74% of wind reports had radar volumes collected at a slower rate. *From 2014 to 2020, the median VCP 212 volume scan time increased from 297 to 368 s near tornado reports, from 258 to 297 s near hail reports, and from 259 to 297 s near wind reports.* Overall, the closest radar scanning tornado, hail, and wind events are completing fewer volumes during the event life cycle in more recent years than prior to the implementation of SAILS.

4. Summary and discussion

This study highlights an evolution in how the atmosphere has been scanned by the WSR-88D network in its first decade

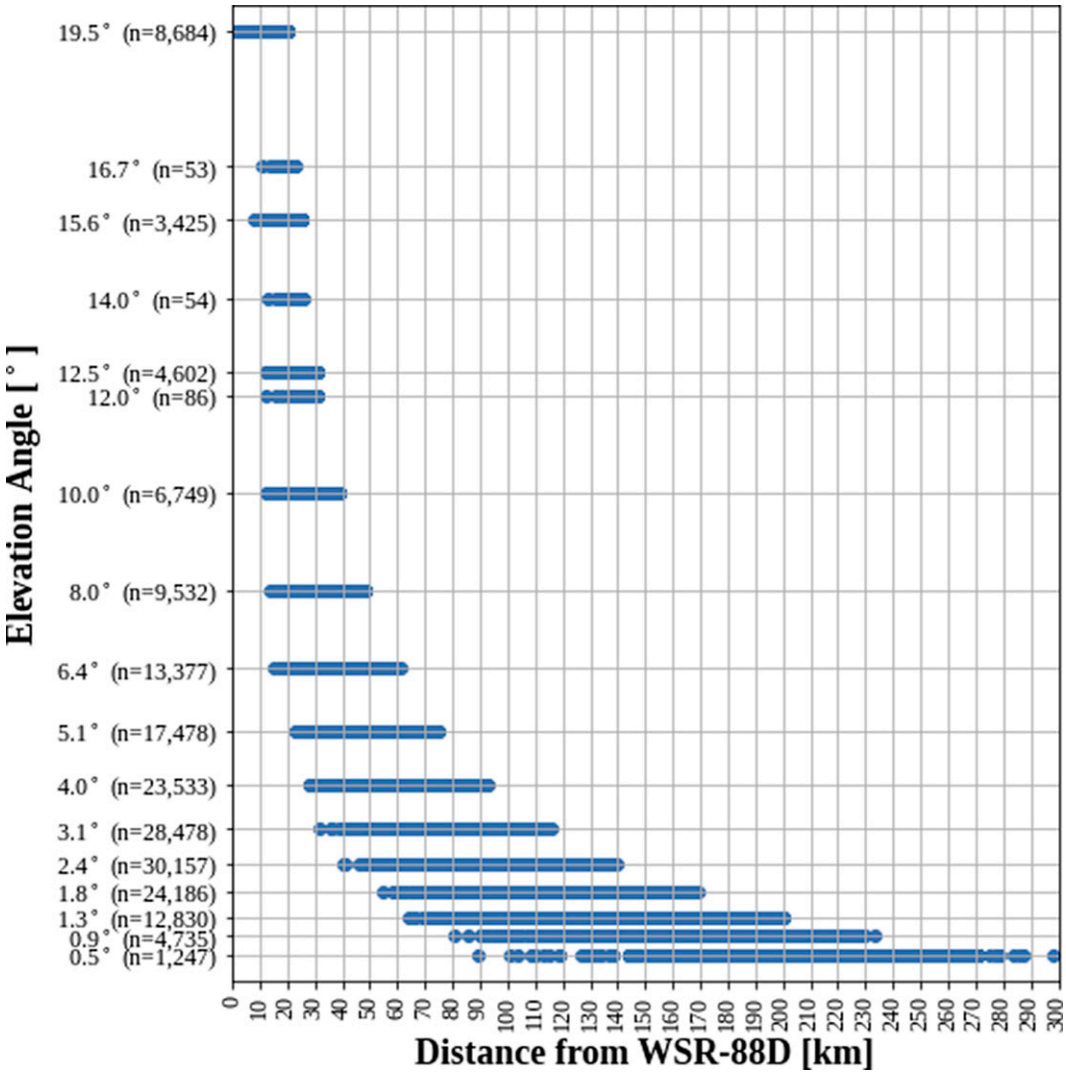

FIG. 11. Radar elevation angle closest to 1 km above the height of the 0°C isothermal level calculated from the RAP analysis grid for 10 177 tornado reports, 56 444 hail reports, and 122 585 thunderstorm wind reports.

of nationwide polarimetric data collection. One area of consistency over the last decade was the widespread usage of VCPs that provide more dense low-level measurements. VCPs 12 and 212 were used in over 96% of tornado warnings, 93% of severe thunderstorm warnings, and 95% of tornado, wind, and hail reports. It continued to be used in a majority of warning decisions and near storm reports after 2018 when VCP 215, which provides more dense radar sampling at mid- to upper levels of the atmosphere and improved data quality, was implemented.

The national implementation of SAILS, MESO-SAILS, and MRLE strategies starting in 2014 marks a distinct shift in measurement priorities that can be beneficial for some endeavors (i.e., warning operations) and potentially harmful to others (i.e., mid- to upper-level atmospheric measurements). Options to add up to three extra low-level scans or an extra scan of each of the four lowest angles (0.5°, 0.9°, 1.3°, and 1.8°) provide more event-specific configurability to these widely used VCPs. SAILSx3, which provides four total lowest-level scans in a single radar volume, was most widely used in tornado warning operations while SAILSx1 was used most frequently in severe thunderstorm warning operations.

From a NWS warning performance perspective, severe thunderstorm and tornado warning decisions issued on convective events with SAILSx2 or SAILSx3 activated had a higher POD and lower FAR than warning scenarios where SAILSx1 or No SAILS were used. Furthermore, events scanned with radars producing more low-level scans typically had warnings issued for them with a greater probability of a positive lead time. This is at least strong circumstantial evidence that more low-level scans of the atmosphere are providing forecasters with better information to make a warning decision, but we caution that this is just one technological variable in the warning decision-making process. NWS offices

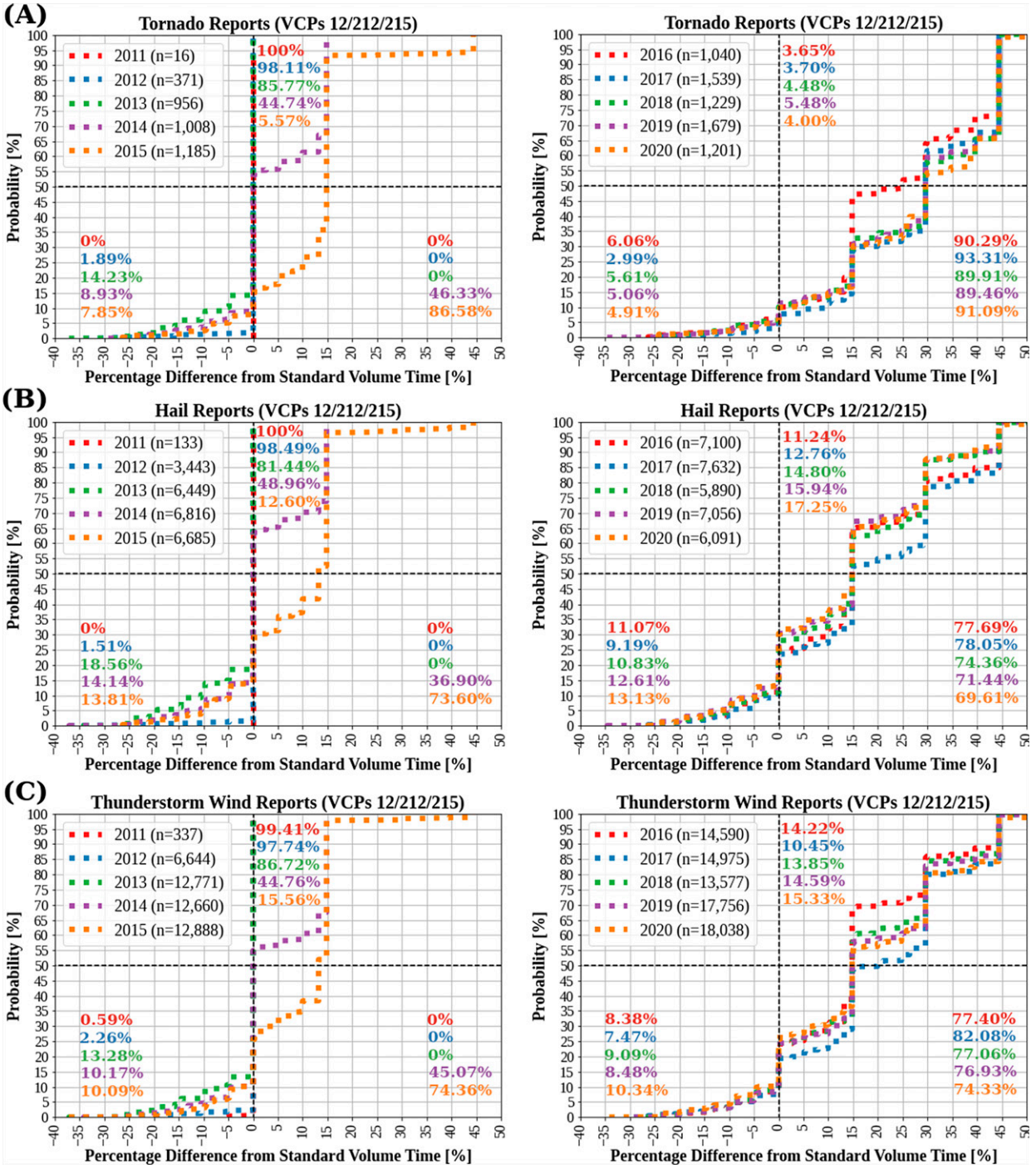

FIG. 12. Cumulative distribution function plots of the percentage decrease or increase in volume scan time for the closest radar volume to a (a) tornado, (b) hail, and (c) thunderstorm wind report (left) from 2011 to 2015 and (right) from 2016 to 2020.

also have access to MRMS which blends information from multiple radars to provide a 3D cube of reflectivity and height-based composite products with a 2-min update rate (Smith et al. 2016; Zhang et al. 2016). These derived radar fields may be used to fill in the gaps to examine what is occurring at midlevels (e.g., using reflectivity at −20°C level to diagnose hail growth potential). Widespread use of MRMS could explain the lack of a decline in severe thunderstorm warning performance where midlevel precursor signatures are more important as an initial part of the severe thunderstorm warning decision-making process.

Other factors, including ambient near-storm environmental conditions, ground truth observations, office warning strategy,

and human expertise can foster a work environment where more confident warning decisions are made (Andra et al. 2002). *We emphasize in particular that there may be a selection bias impact on the performance numbers.* For example, on days in which tornado outbreaks are predicted, forecasters may be more prepared and inclined to employ increased low-level scans. Since severe weather is anticipated on these days, there may be more or better data (e.g., 1800 UTC soundings), increased staffing, or other advantages that lead to better warning performance.

Our attempt to quantify this effect was a comparison of supplemental low-level strategy selection within SPC watches. Since 2016, SAILSx3 was the most used strategy during both severe thunderstorm and tornado warning operations when a tornado watch was issued and a No SAILS strategy was more prominent when no watch was issued. This supports the idea that forecasters may be more likely to use SAILS or MRLE strategies when organized thunderstorms capable of producing widespread wind, hail, or tornadoes are anticipated. Furthermore, it has recently been shown that tornado warnings and events inside SPC watches with a higher severity have a higher POD and lower FAR (Krocak and Brooks 2021). Examining warnings outside of SPC watches revealed a greater percentage of warnings issued near a radar running SAILSx2 or SAILSx3 were verified by a storm report compared to SAILSx1 or No SAILS. However, isolated convection over a localized area may not warrant the issuance of a SPC watch product and the thunderstorm risk information that would cause an NWS office to choose MESO-SAILS could be conveyed through a Convective Outlook or Mesoscale Discussion. Future work should address to what extent the use of SAILS and MRLE are directly responsible for increased warning skill, though isolating the exact impact of additional low-level scanning may be impossible given the large number of variables inherent to issuing warnings. An additional idea worth exploring is whether forecasters may benefit from more aggressive adjustments in implementing SAILS or MRLE in highly conditional or other low probability severe weather situations that are not as well predicted.

Each year since the availability of SAILS, 90% of reported tornadoes and around 75% of hail and wind reports had its closest radar scanning with SAILS. Including polarimetric data observations of hazards before SAILS existed, 76% of significant tornadoes and around 64% of significant hail and wind reports were scanned with some form of SAILS or MRLE activated. Depending on the layer of the atmosphere being examined, this could provide more frequent or less frequent temporal updates of a region of interest. For analyses of mid- to upper-level atmospheric features using dual-polarization radar, there may be up to 33% fewer observations at these levels when data from 2016 and beyond are included. This could hinder the creation of new conceptual models of thunderstorm microphysical processes or climatologies of midlevel thunderstorm features (i.e., Z_{DR} columns, bounded weak echo region heights) as cases from more recent years are included. Indeed, recent work has shown that running a WSR-88D in "rapid-scan" mode provided a more complete picture of Z_{DR} column evolution and would likely provide forecasters more time to anticipate severe hazards (Kuster et al. 2020).

But our view, based on these data, is that while the usage of supplemental low-level scanning strategies is optional, the NWS mission of protecting lives and property on the ground supersedes the scientific benefits of more rapid observations at mid- to upper levels of the atmosphere. Possible solutions to boost volume scan times include the installation of more gap-filling radars to provide more frequent updates of a single storm from equidistant radar sites. Another option would be to implement other rapid-scan radar technologies that would provide full volumes of radar data at faster speeds (e.g., Heinselman et al. 2008; Torres and Schvartzman 2020; Weber et al. 2021). This second option may be more feasible when the WSR-88D network reaches the end of its service life; however, the NEXRAD Service Life Extension Program is ongoing to keep the WSR-88D network maintained through 2040 (Nai et al. 2020).

We interpret the evidence presented in this paper as supporting the continued or even expanded usage of SAILS strategies during severe weather operations, especially for tornado warnings. However, we recommend that NWS offices take into consideration the anticipated hazards and the part of the atmosphere that should best be sampled to provide relevant information when forecasting and nowcasting thunderstorms. For instance, running a SAILS strategy with a high-based thunderstorm close to the radar may undershoot a potentially tornadic rotational signature resulting in a slower return interval of more important upper-level diagnostic features. The usage of MRLE may lessen the potential of this occurring but would also cause even slower radar updates at higher elevation angles, particularly close to the radar. In environments where downbursts are possible, opting for a lower SAILS selection or no SAILS could provide more information to identify a midlevel convergence signature. Examining severe thunderstorm warnings and hail or wind events revealed similar forecast performance when either SAILSx2 or SAILSx3 was used. One fewer low-level scan could save between 31 and 38 s on the overall volume time when in VCP 12 or 212. Overall, making more strategic VCP and SAILS selection decisions, without compromising public safety, could provide improved vertical sampling coverage that researchers and algorithm developers need to better understand the dynamical and microphysical characteristics of thunderstorms and their attendant hazards.

Acknowledgments. This study was supported by NSF Grant AGS-1748191 (Kingfield) and AGS-1748177 (French). The authors thank Dr. David Gagne for his help in the development of the ROC plots and the three reviewers for their helpful improvements.

Data availability statement. The NWS warning and storm report data are available on the NWS Performance Management Web Portal (https://verification.nws.noaa.gov). The Storm Prediction Center watch data are available from the NOAA Storm Prediction Center website (https://www.spc.noaa.gov). The NEXRAD Level-II data are available on the

Amazon S3 Explorer (https://s3.amazonaws.com/noaa-nexrad-level2/index.html) and the National Centers for Environmental Information Archive Information Request System (https://www.ncei.noaa.gov/has/HAS.DsSelect).

REFERENCES

Andra, D. L., Jr., E. M. Quoetone, and W. F. Bunting, 2002: Warning decision making: The relative roles of conceptual models, technology, strategy, and forecaster expertise on 3 May 1999. *Wea. Forecasting*, **17**, 559–566, https://doi.org/10.1175/1520-0434(2002)017<0559:WDMTRR>2.0.CO;2.

Ansari, S., and Coauthors, 2018: Unlocking the potential of NEXRAD data through NOAA's Big Data partnership. *Bull. Amer. Meteor. Soc.*, **99**, 189–204, https://doi.org/10.1175/BAMS-D-16-0021.1.

Benjamin, S. G., and Coauthors, 2016: A North American hourly assimilation and model forecast cycle: The Rapid Refresh. *Mon. Wea. Rev.*, **144**, 1669–1694, https://doi.org/10.1175/MWR-D-15-0242.1.

Bieringer, P., and P. S. Ray, 1996: A comparison of tornado warning lead times with and without NEXRAD Doppler radar. *Wea. Forecasting*, **11**, 47–52, https://doi.org/10.1175/1520-0434(1996)011<0047:ACOTWL>2.0.CO;2.

Black, A. W., and W. S. Ashley, 2011: The relationship between tornadic and nontornadic wind fatalities and warnings. *Wea. Climate Soc.*, **3**, 31–47, https://doi.org/10.1175/2010WCAS1094.1.

Bowden, K. A., and P. L. Heinselman, 2016: A qualitative analysis of NWS forecasters' use of phased-array radar data during severe hail and wind events. *Wea. Forecasting*, **31**, 43–55, https://doi.org/10.1175/WAF-D-15-0089.1.

——, ——, D. M. Kingfield, and R. P. Thomas, 2015: Impacts of phased-array radar data on forecaster performance during severe hail and wind events. *Wea. Forecasting*, **30**, 389–404, https://doi.org/10.1175/WAF-D-14-00101.1.

Brown, R. A., V. T. Wood, R. M. Steadham, R. R. Lee, B. A. Flickinger, and D. Sirmans, 2005: New WSR-88D volume coverage pattern 12: Results of field tests. *Wea. Forecasting*, **20**, 385–393, https://doi.org/10.1175/WAF848.1.

Chrisman, J. N., 2009: Automated Volume Scan Evaluation and Termination (AVSET)—A simple technique to achieve faster volume scan updates. *34th Conf. on Radar Meteorology*, Williamsburg, VA, Amer. Meteor. Soc., P4.4, https://ams.confex.com/ams/34Radar/techprogram/paper_155324.htm.

——, 2013: Dynamic scanning. *NEXRAD Now*, **22**, 1–3, https://www.roc.noaa.gov/WSR88D/PublicDocs/NNOW/NNow22c.pdf.

——, 2014: Multiple elevation scan option for SAILS (MESO-SAILS)—The next step in dynamic scanning for the WSR-88D. Radar Operations Center, 27 pp., https://www.roc.noaa.gov/wsr88d/PublicDocs/NewTechnology/MESO-SAILS_Description_Briefing_Jan_2014.pdf.

——, 2016: Mid-volume rescan of low-level elevations (MRLE): A new approach to enhance sampling of quasi-linear convective systems (QLCSs). New Radar Technologies Web Page, NOAA/NWS/Radar Operations Center, 21 pp., https://www.roc.noaa.gov/WSR88D/PublicDocs/NewTechnology/DQ_QLCS_MRLE_June_2016.pdf.

Crum, T. D., R. L. Alberty, and D. W. Burgess, 1993: Recording, archiving, and using WSR-88D data. *Bull. Amer. Meteor. Soc.*, **74**, 645–653, https://doi.org/10.1175/1520-0477(1993)074<0645:RAAUWD>2.0.CO;2.

——, R. E. Saffle, and J. W. Wilson, 1998: An update on the NEXRAD program and future WSR-88D support to operations. *Wea. Forecasting*, **13**, 253–262, https://doi.org/10.1175/1520-0434(1998)013<0253:AUOTNP>2.0.CO;2.

Daniel, A. E., J. N. Chrisman, C. A. Ray, S. D. Smith, and M. W. Miller, 2014: New WSR-88D operational techniques: Responding to recent weather events. *Proc. 30th Conf. on Environmental Information Processing Technologies*, Atlanta, GA, Amer. Meteor. Soc., 5.2, https://ams.confex.com/ams/94Annual/webprogram/Paper241216.html.

Deierling, W., and W. A. Petersen, 2008: Total lightning activity as an indicator of updraft characteristics. *J. Geophys. Res.*, **113**, 2156–2202, https://doi.org/10.1029/2007JD009598.

Efron, B., 1979: Bootstrap methods: Another look at the jackknife. *Ann. Stat.*, **7**, 1–26, https://doi.org/10.1214/aos/1176344552.

Eilts, M. D., J. T. Johnson, E. D. Mitchell, R. J. Lynn, P. Spencer, S. Cobb, and T. M. Smith, 1996: Damaging downburst prediction and detection algorithm for the WSR-88D. Preprints, *18th Conf. on Severe Local Storms*, San Francisco, CA, Amer. Meteor. Soc., 541–545.

Emmerson, S. W., S. E. Nelson, and A. K. Baker, 2019: A comprehensive analysis of tornado debris signatures associated with significant tornadoes from 2010–2017. *18th Annual Student Conf.*, Phoenix, AZ, Amer. Meteor. Soc., S210, https://ams.confex.com/ams/2019Annual/webprogram/Paper356019.html.

French, M. M., and D. M. Kingfield, 2021: Tornado formation and intensity prediction using polarimetric radar estimates of updraft area. *Wea. Forecasting*, **36**, 2211–2231, https://doi.org/10.1175/WAF-D-21-0087.1.

Gibbs, J. G., 2016: A skill assessment of techniques for real-time diagnosis and short-term prediction of tornado intensity using the WSR-88D. *J. Oper. Meteor.*, **4**, 170–181, https://doi.org/10.15191/nwajom.2016.0413.

Heinselman, P. L., D. L. Priegnitz, K. L. Manross, T. M. Smith, and R. W. Adams, 2008: Rapid sampling of severe storms by the National Weather Radar Testbed phased array radar. *Wea. Forecasting*, **23**, 808–824, https://doi.org/10.1175/2008WAF2007071.1.

Helmus, J. J., and S. M. Collis, 2016: The Python ARM Radar Toolkit (Py-ART), a library for working with weather radar data in the Python Programming Language. *J. Open Res. Software*, **4**, e25, https://doi.org/10.5334/jors.119.

Houser, J. L., H. B. Bluestein, and J. C. Snyder, 2015: Rapid-scan, polarimetric, Doppler radar observations of tornadogenesis and tornado dissipation in a tornadic supercell: The "El Reno, Oklahoma" storm of 24 May 2011. *Mon. Wea. Rev.*, **143**, 2685–2710, https://doi.org/10.1175/MWR-D-14-00253.1.

Hubbert, J. C., V. N. Bringi, L. D. Carey, and S. Bolen, 1998: CSU-CHILL polarimetric radar measurements from a severe hail storm in eastern Colorado. *J. Appl. Meteor.*, **37**, 749–775, https://doi.org/10.1175/1520-0450(1998)037<0749:CCPRMF>2.0.CO;2.

——, M. Dixon, and S. M. Ellis, 2009: Weather radar ground clutter. Part II: Real-time identification and filtering. *J. Atmos. Oceanic Technol.*, **26**, 1181–1197, https://doi.org/10.1175/2009JTECHA1160.1.

Ice, R. L., J. G. Cunningham, J. N. Chrisman, W. D. Zittel, S. D. Smith, O. E. Boydstun, R. D. Cook, and A. K. Heck, 2013: WSR-88D program data quality and efficiency enhancements—Plans and status. *36th Conf. on Radar Meteorology*, Breckenridge, CO, Amer. Meteor. Soc., 368, https://ams.confex.com/ams/36Radar/webprogram/Manuscript/Paper228782/NEXRAD_DQ_Plans_and_Status_Ice_36thRadar_Sept2013_rv2.pdf.

Illingworth, A. J., J. W. F. Goddard, and S. M. Cherry, 1987: Polarization radar studies of precipitation development in convective storms. *Quart. J. Roy. Meteor. Soc.*, **113**, 469–489, https://doi.org/10.1002/qj.49711347604.

Istok, M. J., A. Cheek, A. D. Stern, R. E. Saffle, W. M. Blanchard, B. R. Klein, and N. Shen, 2009: Leveraging multiple FAA radars for NWS operations. *25th Conf. on Int. Interactive Information and Processing Systems (IIPS) for Meteorology, Oceanography, and Hydrology*, Phoenix, AZ, Amer. Meteor. Soc., 10B.2, https://ams.confex.com/ams/89annual/techprogram/paper_145466.htm.

——, D. W. Burgess, R. L. Ice, M. Jain, R. L. Murnan, and J. A. Schultz, 2017: NEXRAD product improvement—Update 2017. *33rd Conf. on Environmental Information Processing Technologies*, Seattle, WA, Amer. Meteor. Soc., 9A.1, https://ams.confex.com/ams/97Annual/webprogram/Paper315526.html.

Krause, J. M., 2016: A simple algorithm to discriminate between meteorological and nonmeteorological radar echoes. *J. Atmos. Oceanic Technol.*, **33**, 1875–1885, https://doi.org/10.1175/JTECH-D-15-0239.1.

Krocak, M. J., and H. E. Brooks, 2021: The influence of weather watch type on the quality of tornado warnings and its implications for future forecasting systems. *Wea. Forecasting*, **36**, 1675–1680, https://doi.org/10.1175/WAF-D-21-0052.1.

Kumjian, M. R., and A. V. Ryzhkov, 2008: Polarimetric signatures in supercell thunderstorms. *J. Appl. Meteor. Climatol.*, **47**, 1940–1961, https://doi.org/10.1175/2007JAMC1874.1.

——, A. P. Khain, N. Benmoshe, E. Ilotoviz, A. V. Ryzhkov, and V. T. J. Phillips, 2014: The anatomy and physics of Z_{DR} columns: Investigating a polarimetric radar signature with a spectral bin microphysical model. *J. Appl. Meteor. Climatol.*, **53**, 1820–1843, https://doi.org/10.1175/JAMC-D-13-0354.1.

Kurdzo, J. M., D. J. Bodine, B. L. Cheong, and R. D. Palmer, 2015: High-temporal resolution polarimetric X-band Doppler radar observations of the 20 May 2013 Moore, Oklahoma, tornado. *Mon. Wea. Rev.*, **143**, 2711–2735, https://doi.org/10.1175/MWR-D-14-00357.1.

Kuster, C. M., J. C. Snyder, T. J. Schuur, T. T. Lindley, P. L. Heinselman, J. C. Furtado, J. W. Brogden, and R. Toomey, 2019: Rapid-update radar observations of Z_{DR} column depth and its use in the warning decision process. *Wea. Forecasting*, **34**, 1173–1188, https://doi.org/10.1175/WAF-D-19-0024.1.

——, T. J. Schuur, T. T. Lindley, and J. C. Snyder, 2020: Using Z_{DR} columns in forecaster conceptual models and warning decision-making. *Wea. Forecasting*, **35**, 2507–2522, https://doi.org/10.1175/WAF-D-20-0083.1.

——, B. R. Bowers, J. T. Carlin, T. J. Schuur, J. W. Brogden, R. Toomey, and A. Dean, 2021: Using K_{DP} cores as a downburst precursor signature. *Wea. Forecasting*, **36**, 1183–1198, https://doi.org/10.1175/WAF-D-21-0005.1.

Lakshmanan, V., T. Smith, G. Stumpf, and K. Hondl, 2007: The Warning Decision Support System–Integrated Information. *Wea. Forecasting*, **22**, 596–612, https://doi.org/10.1175/WAF1009.1.

Maddox, R. A., D. S. Zaras, P. L. MacKeen, J. J. Gourley, R. Rabin, and K. W. Howard, 1999: Echo height measurements with the WSR-88D: Use of data from one versus two radars. *Wea. Forecasting*, **14**, 455–460, https://doi.org/10.1175/1520-0434(1999)014<0455:EHMWTW>2.0.CO;2.

Mann, H. B., and D. R. Whitney, 1947: On a test of whether one of two random variables is stochastically larger than the other. *Ann. Math. Stat.*, **18**, 50–60, https://doi.org/10.1214/aoms/1177730491.

Nai, F., J. Boettcher, C. Curtis, D. Schvartzman, and S. Torres, 2020: The impact of elevation sidelobe contamination on radar data quality for operational implementation. *J. Appl. Meteor. Climatol.*, **59**, 707–724, https://doi.org/10.1175/JAMC-D-19-0092.1.

National Academy of Sciences, 2002: *Weather Radar Technology beyond NEXRAD*. National Academy Press, 72 pp.

NOAA, 2011: NWS central region service assessment: Joplin, Missouri, Tornado—May 22, 2011. NOAA, 41 pp., https://www.weather.gov/media/publications/assessments/Joplin_tornado.pdf.

NWS, 2009: Verification procedures: National Weather Services Instruction 10-1601. NOAA/NWS, 83 pp., https://www.nws.noaa.gov/directives/010/archive/pd01016001d.pdf.

——, 2020: WFO severe weather product specification: National Weather Service Instruction 10-511. NOAA/NWS, 64 pp., https://www.nws.noaa.gov/directives/sym/pd01005011curr.pdf.

——, 2021: National severe weather products specification: National Weather Service Instruction 10-512. NOAA/NWS, 73 pp., https://www.nws.noaa.gov/directives/sym/pd01005012curr.pdf.

Ortega, K. L., T. M. Smith, K. L. Manross, K. A. Scharfenberg, A. Witt, A. G. Kolodziej, and J. J. Gourley, 2009: The Severe Hazards Analysis and Verification Experiment. *Bull. Amer. Meteor. Soc.*, **90**, 1519–1530, https://doi.org/10.1175/2009BAMS2815.1.

Picca, J. C., M. R. Kumjian, and A. V. Ryzhkov, 2010: Z_{DR} columns as a predictive tool for hail growth and storm evolution. *25th Conf. on Severe Local Storms*, Denver, CO, Amer. Meteor. Soc., 11.3, https://ams.confex.com/ams/25SLS/techprogram/paper_175750.htm.

Polger, P. D., B. S. Goldsmith, R. C. Przywarty, and J. R. Bocchieri, 1994: National Weather Service warning performance based on the WSR-88D. *Bull. Amer. Meteor. Soc.*, **75**, 203–214, https://doi.org/10.1175/1520-0477(1994)075<0203:NWSWPB>2.0.CO;2.

Richardson, L. M., J. G. Cunningham, W. D. Zittel, R. R. Lee, R. L. Ice, V. M. Melnikov, N. P. Hoban, and J. G. Gebauer, 2017: Bragg scatter detection by the WSR-88D. Part I: Algorithm development. *J. Atmos. Oceanic Technol.*, **34**, 465–478, https://doi.org/10.1175/JTECH-D-16-0030.1.

ROC, 2015: WSR-88D Volume Coverage Pattern (VCP) improvement initiatives. New Radar Technologies Web Page, NOAA/NWS/Radar Operations Center, 8 pp., https://www.roc.noaa.gov/WSR88D/PublicDocs/NewTechnology/New_VCP_Paradigm_Public_Oct_2015.pdf.

Ryzhkov, A. V., T. J. Schuur, D. W. Burgess, and D. S. Zrnić, 2005: Polarimetric tornado detection. *J. Appl. Meteor.*, **44**, 557–570, https://doi.org/10.1175/JAM2235.1.

——, M. R. Kumjian, S. M. Ganson, and P. Zhang, 2013: Polarimetric radar characteristics of melting hail. Part II: Practical implications. *J. Appl. Meteor. Climatol.*, **52**, 2871–2886, https://doi.org/10.1175/JAMC-D-13-074.1.

Sachidananda, M., and D. S. Zrnić, 1999: Systematic phase codes for resolving range overlaid signals in a Doppler weather radar. *J. Atmos. Oceanic Technol.*, **16**, 1351–1363, https://doi.org/10.1175/1520-0426(1999)016<1351:SPCFRR>2.0.CO;2.

Saffle, R., M. Istok, and L. D. Johnson, 2002: NEXRAD open systems—Progress and plans. Preprints, *18th Conf. on Interactive Information Processing Systems*, Orlando, FL, Amer. Meteor. Soc., 5.1.

Smalley, D. J., B. J. Bennett, and R. S. Frankel, 2005: MIGFA: The Machine Intelligent Gust Front Algorithm for NEXRAD. *32nd Conf. on Radar Meteorology*, Albuquerque, NM,

Amer. Meteor. Soc., 8R.4., https://ams.confex.com/ams/32Rad11Meso/techprogram/paper_96098.htm.

Smith, B. T., R. L. Thompson, J. S. Grams, C. Broyles, and H. E. Brooks, 2012: Convective modes for significant severe thunderstorms in the contiguous United States. Part I: Storm classification and climatology. *Wea. Forecasting*, **27**, 1114–1135, https://doi.org/10.1175/WAF-D-11-00115.1.

Smith, T. M., and Coauthors, 2016: Multi-Radar Multi-Sensor (MRMS) severe weather and aviation products: Initial operating capabilities. *Bull. Amer. Meteor. Soc.*, **97**, 1617–1630, https://doi.org/10.1175/BAMS-D-14-00173.1.

Snyder, J. C., and A. V. Ryzhkov, 2015: Automated detection of polarimetric tornadic debris signatures using a hydrometeor classification algorithm. *J. Appl. Meteor. Climatol.*, **54**, 1861–1870, https://doi.org/10.1175/JAMC-D-15-0138.1.

——, ——, M. R. Kumjian, A. P. Khain, and J. Picca, 2015: A Z_{DR} column detection algorithm to examine convective storm updrafts. *Wea. Forecasting*, **30**, 1819–1844, https://doi.org/10.1175/WAF-D-15-0068.1.

Stumpf, G. J., A. Witt, E. D. Mitchell, P. L. Spencer, J. T. Johnson, M. D. Eilts, K. W. Thomas, and D. W. Burgess, 1998: The National Severe Storms Laboratory mesocyclone detection algorithm for the WSR-88D. *Wea. Forecasting*, **13**, 304–326, https://doi.org/10.1175/1520-0434(1998)013<0304:TNSSLM>2.0.CO;2.

Torres, S. M., and C. D. Curtis, 2007: Initial implementation of super-resolution data on the NEXRAD network. *23rd Conf. on Information Processing Systems*, San Antonio, TX, Amer. Meteor. Soc., 5B.10, https://ams.confex.com/ams/87ANNUAL/techprogram/paper_116240.htm.

——, and D. Schvartzman, 2020: A simulation framework to support the design and evaluation of adaptive scanning for phased-array weather radars. *J. Atmos. Oceanic. Technol.*, **37**, 2321–2339, https://doi.org/10.1175/JTECH-D-20-0087.1.

Trapp, R. J., D. M. Wheatley, N. T. Atkins, R. W. Przybylinski, and R. Wolf, 2006: Buyer beware: Some words of caution on the use of severe wind reports in postevent assessment and research. *Wea. Forecasting*, **21**, 408–415, https://doi.org/10.1175/WAF925.1.

Van Den Broeke, M. S., 2017: Polarimetric radar metrics related to tornado life cycles and intensity in supercell storms. *Mon. Wea. Rev.*, **145**, 3671–3686, https://doi.org/10.1175/MWR-D-16-0453.1.

van Lier-Walqui, M., and Coauthors, 2016: On polarimetric radar signatures of deep convection for model evaluation: Column of specific differential phase observed during MC3E. *Mon. Wea. Rev.*, **144**, 737–758, https://doi.org/10.1175/MWR-D-15-0100.1.

Weber, M., and Coauthors, 2021: Towards the next generation operational meteorological radar. *Bull. Amer. Meteor. Soc.*, **102**, E1357–E1383, https://doi.org/10.1175/BAMS-D-20-0067.1.

Wilson, K. A., P. L. Heinselman, C. M. Kuster, D. M. Kingfield, and Z. Kang, 2017: Forecaster performance and workload: Does radar update time matter? *Wea. Forecasting*, **32**, 253–274, https://doi.org/10.1175/WAF-D-16-0157.1.

Witt, A., M. D. Eilts, G. J. Stumpf, J. T. Johnson, E. D. W. Mitchell, and K. W. Thomas, 1998a: An enhanced hail detection algorithm for the WSR-88D. *Wea. Forecasting*, **13**, 286–303, https://doi.org/10.1175/1520-0434(1998)013<0286:AEHDAF>2.0.CO;2.

——, ——, ——, E. D. Mitchell, J. T. Johnson, and K. W. Thomas, 1998b: Evaluating the performance of WSR-88D severe storm detection algorithms. *Wea. Forecasting*, **13**, 513–518, https://doi.org/10.1175/1520-0434(1998)013<0513:ETPOWS>2.0.CO;2.

Zhang, J., and Coauthors, 2016: Multi-Radar Multi-Sensor (MRMS) quantitative precipitation estimation: Initial operating capabilities. *Bull. Amer. Meteor. Soc.*, **97**, 621–638, https://doi.org/10.1175/BAMS-D-14-00174.1.

Zittel, W. D., 2019: Theory and concept of operations for multi-PRF dealiasing algorithm's VCP 112. New Radar Technologies Web Page, NOAA/NWS/Radar Operations Center, 13 pp., https://www.roc.noaa.gov/WSR88D/PublicDocs/NewTechnology/Theory_ConOps_VCP112.pdf.

——, and T. Wiegman, 2005: VCP 121 and the multi-PRF dealiasing algorithm. *NEXRAD Now*, **14**, 9–15, https://www.roc.noaa.gov/wsr88d/PublicDocs/NNOW/NNwinter05d.pdf.